

## Standard Model Higgs boson at ATLAS

E. PETIT on behalf of the ATLAS COLLABORATION

*LAPP, CNRS/IN2P3 and University of Savoie - Annecy-le-Vieux, France*

ricevuto il 20 Giugno 2013; approvato l'1 Luglio 2013

**Summary.** — The ATLAS results on the search and study of the Standard Model Higgs boson with  $5\text{ fb}^{-1}$  of  $\sqrt{s} = 7\text{ TeV}$  and  $13\text{ fb}^{-1}$  of  $\sqrt{s} = 8\text{ TeV}$  data are presented. Analyses in the five main decay channels and their combination are detailed. The spin of the new particle is studied by comparing the data to the SM Higgs boson expectations and to specific spin models.

PACS 14.80.Bn – Standard-model Higgs bosons.

### 1. – Introduction

The ATLAS [1] and CMS [2] collaborations have independently reported observations of a new boson compatible with the SM Higgs boson, using the 2011 and 2012 datasets collected until the end of June 2012 [3, 4]. Nevertheless, this discovery was made with the combination of different decay channels, and the observation had not been confirmed in each channel yet. In order to confirm whether this particle is the Standard Model Higgs boson or not, one has to study its properties: mass, spin and couplings. The last point is detailed in ref. [5].

The results presented here are based on the proton-proton collision datasets corresponding to integrated luminosities of  $4.8\text{ fb}^{-1}$  collected at  $\sqrt{s} = 7\text{ TeV}$  and  $13\text{ fb}^{-1}$  collected at  $\sqrt{s} = 8\text{ TeV}$ .

The following note is organised as follows: since the mass of the discovered particle is around  $125\text{ GeV}$ , many decay channels can be used to study its properties, the main ones being described below, in decreasing order of sensitivity:  $H \rightarrow ZZ^{(*)} \rightarrow llll$ ,  $H \rightarrow \gamma\gamma$ ,  $H \rightarrow WW^{(*)} \rightarrow \ell\nu\ell\nu$ ,  $H \rightarrow \tau\tau$  and  $H \rightarrow b\bar{b}$ . The combination of these channels and the mass and spin determinations of the new boson are then described.

### 2. – $H \rightarrow ZZ^{(*)}$

The  $H \rightarrow ZZ^{(*)} \rightarrow llll$  channel [6] is often referred to as the “golden channel” because of its high signal-over-background ratio, close to unity, even if it suffers from a small number of expected signal events. The search is based on the selection of two same flavour, opposite sign lepton pairs. The four leptons are required to be well identified and

TABLE I. – Number of expected  $H \rightarrow ZZ^{(*)}$  signal and background events as well as the number of observed events in a 120–130 GeV window for the combined  $\sqrt{s} = 8$  TeV and  $\sqrt{s} = 7$  TeV datasets [6].

	$4\mu$	$2e2\mu$	$2\mu2e$	$4e$	Total
Signal	4.0	2.4	1.7	1.8	9.9
$ZZ^{(*)}$	2.0	1.0	0.7	0.9	4.7
$Z, Zb\bar{b}, t\bar{t}$	0.4	0.3	1.2	1.7	3.6
Observed	8	4	2	4	18

isolated with  $p_T > 20, 15, 10$  and  $7$  (electron)/ $6$  (muon) GeV respectively. The lepton pair with invariant mass closest to the  $Z$  boson mass must have an invariant mass  $m_{12}$  between 50 and 106 GeV. The requirement on the other lepton pair is relaxed because the second  $Z$  boson must be off-shell for a 125 GeV Higgs boson; its invariant mass  $m_{34}$  has to be between 17.5 and 115 GeV.

The irreducible background  $ZZ^{(*)}$  is estimated from the Monte-Carlo prediction and normalised to the theoretical cross section. The reducible background, mainly  $Z +$  jets and  $t\bar{t}$ , is estimated from data-driven measurements, depending of the flavour of the sub-leading lepton pair. If the subleading pair is made of muon, the irreducible background dominates whereas the reducible background does in the case of a sub-leading electron pair, as seen in table I.

The number of expected and observed events summarised in table I shows that the total number of expected events is in good agreement with the observed events, meaning that an excess over the background hypothesis is seen. The significance of this excess is quantified by the probability  $p_0$  that a background only experiment is more signal-like than the observed data. For the combined dataset, the observed minimum  $p_0$  value correspond to a significance of  $4.1\sigma$  for an expected value of  $3.1\sigma$  (fig. 1, left). The signal strength at this mass, defined as the ratio between the observed and expected number of signal events, is  $1.3_{-0.4}^{+0.5}$ , in good agreement with the Standard Model expectation.

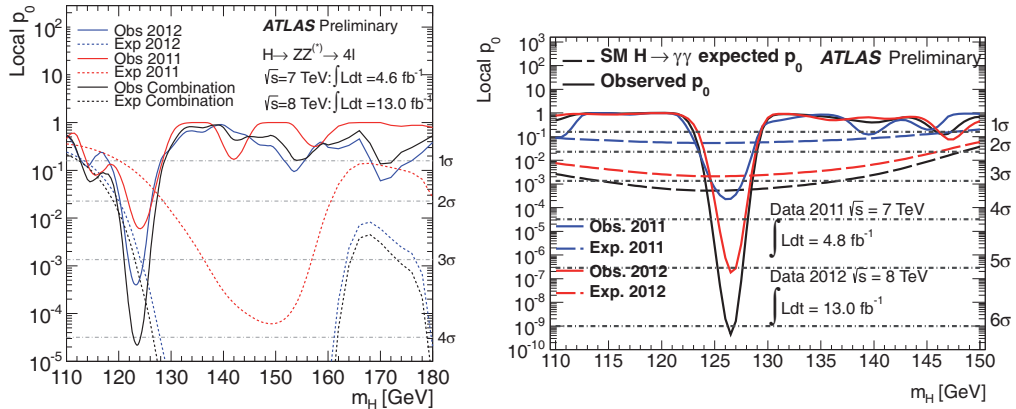


Fig. 1. – Observed local  $p_0$  for the  $H \rightarrow ZZ^{(*)} \rightarrow \ell\ell\ell\ell$  channel (left) [6] and the  $H \rightarrow \gamma\gamma$  channel (right) [7]. Both plots correspond to the combination of the  $\sqrt{s} = 7$  TeV and  $\sqrt{s} = 8$  TeV datasets.

### 3. – $H \rightarrow \gamma\gamma$

In the  $H \rightarrow \gamma\gamma$  channel [7], a few hundreds signal events are expected, but this channel has to deal with a large irreducible ( $\gamma\text{-}\gamma$ ) and reducible ( $\gamma\text{-}jet$  and  $dijet$ ) background, with a signal over background ratio of a few percent for the inclusive selection. Two well identified and isolated photon with  $E_T > 40$  and  $30$  GeV are required. The fraction of genuine diphoton events is around 75%.

In order to increase the sensitivity, the dataset is divided in 12 exclusive categories with different signal over background ratios (from 0.014 to 0.204) and different diphoton invariant mass resolutions (from 1.4 to 2.5 GeV). Nine categories are based on the centrality of the photons, on their conversion state, and on the diphoton transverse momentum orthogonal to the diphoton thrust axis in the transverse plane<sup>(1)</sup>. In addition, a category is enriched in vector boson fusion process, and for the  $\sqrt{s} = 8$  TeV dataset, two categories are enriched in associated production with a vector boson.

The observed local  $p_0$  value for the combined  $\sqrt{s} = 7$  TeV and  $\sqrt{s} = 8$  TeV dataset corresponds to a significance of  $6.1 \sigma$  at 126.5 GeV while the expectation was  $3.3 \sigma$ . The observation of the new particle is thus confirmed in the di-photon channel alone (fig. 1, right). The observed (expected) significance is also  $5.1$  ( $2.9$ )  $\sigma$  for the  $\sqrt{s} = 8$  TeV dataset alone. The best fit of the signal strength for a mass of 126.6 GeV is  $1.80 \pm 0.30(\text{stat.})_{-0.15}^{+0.21}(\text{syst.})_{-0.14}^{+0.20}(\text{theory})$ . This value corresponds to a difference of 2.2 standard deviation from the Standard Model Higgs boson signal hypothesis.

### 4. – $H \rightarrow WW^{(*)}$

In the  $H \rightarrow WW^{(*)}$  channel [8], a few tens of signal events are expected, with a signal over background ratio of around 10%; but because of the presence of neutrinos in the final state, it is not possible to reconstruct completely the event. The transverse mass constructed from the leptons and the missing transverse energy is used as the discriminating variable. The current analysis was made with  $\sqrt{s} = 8$  TeV and in the  $e\nu\mu\nu$  final state only. This allows to reject a lot of Drell-Yan background, and provides most of the sensitivity. Two leading good isolated leptons with a transverse momentum larger than 25 and 15 GeV respectively are selected. Several cuts are made to reject the Drell-Yan and  $t\bar{t}$  backgrounds, such as cuts on the missing transverse energy or the transverse mass of the leptons. Cuts are also made to separate between  $WW$  and Higgs boson events, making use of the spin correlations: the leptons tend to be emitted in the same direction for the latter case. The transverse mass  $m_{\ell\ell}$  is required to be lower than 50 GeV and the difference between the azimuthal angles of the leptons  $\Delta\varphi_{\ell\ell}$  to be lower than 1.8.

The events are then divided in two categories: the 0-jet category which is dominated by  $WW$  background events and the 1-jet category which is dominated by top background events.

The number of background events in each category is extracted using shapes from Monte Carlo events and normalised to the number of events in data in control regions enriched in the targeted background. The number of expected signal and background events

---

<sup>(1)</sup>  $p_{Tt} = |\vec{p}_T^{\gamma\gamma} \times \hat{t}|$ , where  $\hat{t} = \frac{\vec{p}_T^{\gamma 1} - \vec{p}_T^{\gamma 2}}{|\vec{p}_T^{\gamma 1} - \vec{p}_T^{\gamma 2}|}$  denotes the transverse thrust,  $\vec{p}_T^{\gamma 1}$  and  $\vec{p}_T^{\gamma 2}$  are the transverse momenta of the two photons, and  $\vec{p}_T^{\gamma\gamma} = \vec{p}_T^{\gamma 1} + \vec{p}_T^{\gamma 2}$  is the transverse momentum of the diphoton system.

TABLE II. – Observed numbers of  $H \rightarrow WW^{(*)}$  events compared to the expectation from signal ( $m_H = 125$  GeV) and background after the full event selection, including a cut on the transverse mass of  $0.75 m_H < m_T < m_H$  [8].

	Signal	WW	Top	Others	Total bkg	Observed
$H + 0$ jet	$45 \pm 9$	242	27	64	$334 \pm 28$	423
$H + 1$ jet	$18 \pm 6$	40	50	23	$114 \pm 18$	141

as well as the number of observed events are summarised in table II. An excess of events with respect to the background only hypothesis can be seen, illustrated on fig. 2, left.

Figure 2, right shows the  $p_0$  value of the combined analysis. A broad excess for a Higgs boson mass lower than 150 GeV is seen. The corresponding observed (expected) significance for a mass of 125 GeV is  $2.6 \sigma$  ( $1.9 \sigma$ ). The signal strength  $\mu$  is equal to  $1.5 \pm 0.6$ , fully compatible with the Standard Model expectation.

### 5. – $H \rightarrow \tau\tau$

The  $H \rightarrow \tau\tau$  channel [9] benefit from a quite large branching ratio, with around 150 expected reconstructed events, but suffer from a large background from  $Z \rightarrow \tau\tau$  events. The events are divided into different categories, depending on the leptonic or hadronic nature of the decay of the  $\tau$  leptons:  $\tau_{lep}\tau_{lep}$ ,  $\tau_{lep}\tau_{had}$  and  $\tau_{had}\tau_{had}$ . Additional categories enriched in vector boson fusion production mode increase the sensitivity because of the larger signal over background ratio ( $\sim 10\%$  instead of a few per mil). Boosted categories also increases the sensitivity thanks to the improvement of the invariant di-tau mass resolution, allowing a better discrimination between  $Z \rightarrow \tau\tau$  and  $H \rightarrow \tau\tau$  events.

The main background,  $Z \rightarrow \tau\tau$ , is estimated using an embedding technique in which muons from  $Z \rightarrow \mu\mu$  events from data are replaced by taus from the simulation. The effect from additional jets, underlying event and pile-up is then taken from data. The

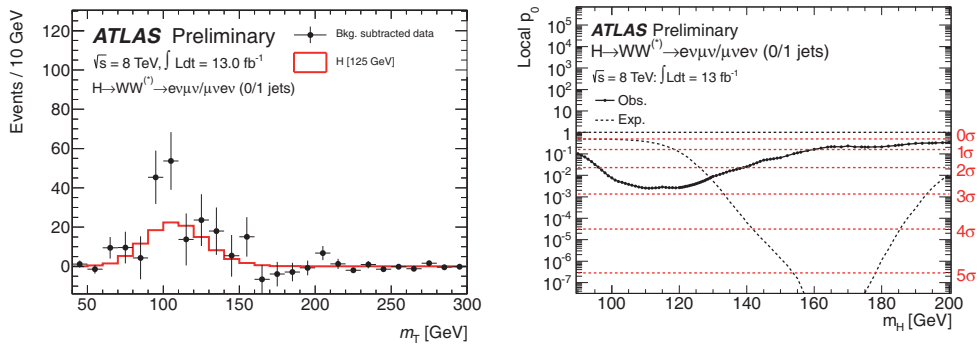


Fig. 2. – On the left,  $m_T$  distribution in data with the estimated background subtracted, overlaid with the predicted signal for  $m_H = 125$  GeV. The distributions are summed for the  $H + 0$ -jet and  $H + 1$ -jet analyses. On the right, observed probability for the background-only scenario as a function of  $m_H$ , as well as the corresponding expectation for the signal+background hypothesis at the given value of  $m_H$  [8].

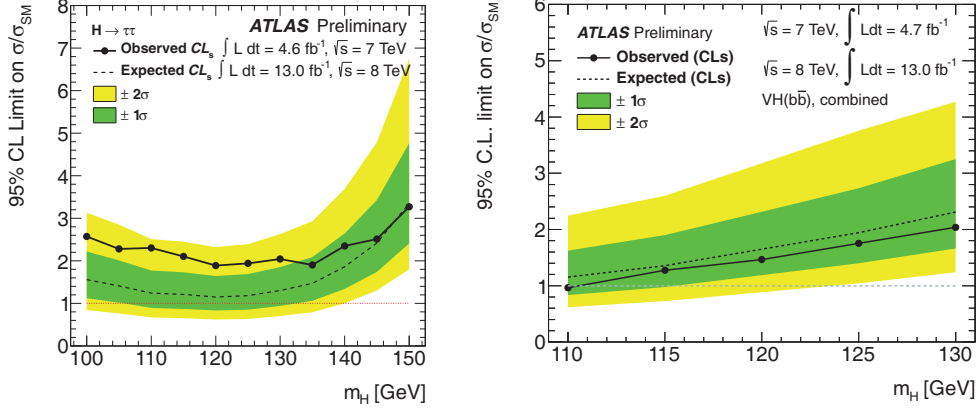


Fig. 3. – Observed and expected 95% confidence level upper limits on the Higgs boson cross-section times branching ratio, normalised to the SM expectation, as a function of the Higgs boson mass. The left plot correspond to the  $H \rightarrow \tau\tau$  analysis [9], and the right plot to the  $H \rightarrow b\bar{b}$  analysis [10]. Both plots correspond to the combination of the  $\sqrt{s} = 7$  TeV and  $\sqrt{s} = 8$  TeV datasets.

reducible background events are estimated from Monte-Carlo samples checked on data in control regions or directly estimated from data.

In this channel, no excess is seen, and an exclusion at 95% CL is estimated, which can be seen in fig. 3, left. For a Higgs boson mass of 125 GeV, the observed (expected) limit is 1.9 (1.2) times the Standard Model expectation. The observed (expected)  $p_0$  value is  $1.1 \sigma$  ( $1.7 \sigma$ ), corresponding to signal strength of  $0.7 \pm 0.7$ .

## 6. – $H \rightarrow b\bar{b}$

The  $H \rightarrow b\bar{b}$  channel [10] benefits from the largest observable branching ratio for a Higgs boson mass of 125 GeV. But because of the large QCD background at the LHC, only the associated production with a gauge boson is considered. Two  $b$  jets are selected with a transverse momentum larger than 45 and 25 GeV respectively, using a  $b$ -tagging algorithm with a signal efficiency of 70% and a light jet rejection of 150 measured on  $t\bar{t}$  events.

The selected events are divided on categories depending on the gauge boson decay: 0 lepton and a high missing transverse energy sensitive to  $Z \rightarrow \nu\nu$  decays, 1 lepton,  $E_{\text{T}}^{\text{miss}}$  and a transverse mass compatible with the  $W$  boson sensitive to  $W \rightarrow \ell\nu$  decays, and 2 jets, low  $E_{\text{T}}^{\text{miss}}$  and an invariant mass compatible with the  $Z$  boson sensitive to the  $Z \rightarrow \ell\ell$  decays. Those events are further divided in categories depending on the presence of extra jets,  $E_{\text{T}}^{\text{miss}}$  or transverse momentum of the gauge boson, with different  $m_{b\bar{b}}$  resolution and signal over background ratio.

The main backgrounds are  $t\bar{t}$  and gauge boson + jets, whose shape is taken from simulation and normalised to data in control samples.

In this channel, no excess is seen, and an exclusion at 95% CL is estimated, which can be seen in fig. 3, right. For a Higgs boson mass of 125 GeV, the observed (expected) limit is 1.8 (1.9) times the Standard Model expectation, corresponding to signal strength of  $-0.4 \pm 0.7(\text{stat.}) \pm 0.8(\text{syst.})$ . This channel is already limited by the systematic uncertainties.

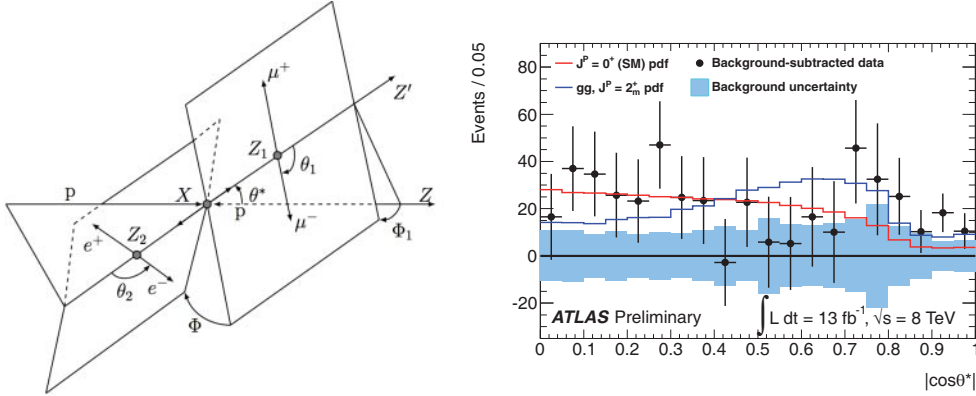


Fig. 4. – On the left, definition of the production and decay angles in an  $X \rightarrow ZZ^{(*)} \rightarrow 4l$  decay. The illustration is drawn with the beam axis in the lab frame, the  $Z_1$  and  $Z_2$  in the  $X$  rest frame and the leptons in their corresponding parent rest frame [6]. On the right, background-subtracted  $\cos\theta^*$  distributions in the diphoton channel are shown, profiled with a fit where the  $0^+/2^+$  ratio is free. The error bars correspond to the data statistical uncertainties only and the blue band shows the background uncertainty before the fit. The two different signal spin shapes are superimposed [7].

## 7. – Combination of channels

All the channels described above are combined [11], leading to an observed significance of  $7.0\sigma$  for an expectation of  $5.9\sigma$ . This excess corresponds to a signal strength of  $1.35 \pm 0.19(\text{stat.}) \pm 0.15(\text{syst.})$ . This value is compatible with the Standard Model expectation.

The mass of the particle is computed from the two high resolution channels. The measured mass for the individual channels are  $123.5 \pm 0.8(\text{stat.}) \pm 0.3(\text{syst.})$  GeV for the  $H \rightarrow ZZ^{(*)}$  channel and  $126.6 \pm 0.3(\text{stat.}) \pm 0.7(\text{syst.})$  GeV for the  $H \rightarrow \gamma\gamma$  channel. The difference between the two measured mass is  $3.0 \pm 0.8(\text{stat.})_{-0.6}^{+0.7}(\text{syst.})$  GeV, corresponding to 2.3 to 2.7 standard deviation depending on how the correlations between the systematic uncertainties are taken into account. The combined mass is  $125.2 \pm 0.3(\text{stat.}) \pm 0.6(\text{syst.})$  GeV.

## 8. – Spin of the boson

In order to probe whether the observed boson is the Standard Model Higgs boson or not, its spin and parity have to be measured. The observation of the  $H \rightarrow \gamma\gamma$  decay strongly disfavours the spin 1 hypothesis under some assumptions because of the Landau-Yang theorem. The observation of fermionic decays ( $H \rightarrow \tau\tau$  and  $H \rightarrow b\bar{b}$ ) would exclude a spin 2 hypothesis.

The models tested in the following are the spin  $0^+$  (Standard Model Higgs boson), spin  $0^-$  (predicted in supersymmetric models),  $2^+$  (graviton-like) and  $2^-$  (pseudo-tensor). For the benchmark spin 2-even model, only minimal couplings and 100% gluon fusion are considered.

In order to distinguish between the different hypothesis, angular correlations between the decays are used, as illustrated in fig. 4 left for the  $H \rightarrow ZZ^{(*)} \rightarrow \ell\ell\ell\ell$  case.

**8.1. Spin in  $H \rightarrow \gamma\gamma$ .** – In this analysis [7], the  $0^+$  and  $2^+$  hypotheses are compared, using the  $\cos\theta^{*(2)}$  distribution. This distribution is supposed to be flat for a spin 0 particle, before acceptance cuts.

The events used for the analysis are taken from the signal region, *ie* with a di-photon invariant mass  $m_{\gamma\gamma}$  between 123.8 and 128.6 GeV. In this region, 199 signal events are expected. The background is determined by fits on the  $m_{\gamma\gamma}$  distribution in bins of  $\cos\theta^*$ . The background-subtracted distribution can be seen in fig. 4, right. The expectations for the two spin hypothesis are also shown, and one can see the clear difference in shape between them.

The compatibility between data and the two different hypotheses is estimated by a likelihood ratio of the  $0^+$  and  $2^+$  signal plus background hypotheses. The expected separation between the two hypotheses is  $1.8\sigma$ , and the observed exclusion of the  $2^+$  hypothesis is at 91% CL whereas the data are compatible with the  $0^+$  hypothesis within  $0.5\sigma$ .

**8.2. Spin in  $H \rightarrow ZZ^{(*)}$ .** – In this analysis [6], four hypotheses spin and parity,  $0^+$ ,  $0^-$ ,  $2^-$  and  $2^+$ , are tested, using the 5 angular variables illustrated in fig. 4 left and the invariant masses of the two  $Z$  bosons. Two methods use these variables, a Boosted Decision Tree (BDT) in a multivariate analysis, and a matrix element based likelihood ratio ( $J^P$ -MELA).

Both methods use events with an invariant mass  $m_{4\ell}$  between 115 and 130 GeV and give compatible results. When comparing the  $2^+$  and  $0^+$  hypotheses, the  $2^+$  hypothesis is excluded at 85% CL (80% expected) whereas the data are compatible with the  $0^+$  hypothesis. When comparing the  $0^+$  and  $0^-$  hypotheses, the  $0^-$  hypothesis is excluded at 99% CL (96% expected) whereas the data are compatible with the  $0^+$  hypothesis within  $0.18\sigma$ .

In all the cases, the data are compatible with the  $0^+$  hypothesis.

## 9. – Conclusions

The ATLAS results with  $5\text{fb}^{-1}$  of  $\sqrt{s} = 7\text{TeV}$  data and  $13\text{fb}^{-1}$  of  $\sqrt{s} = 8\text{TeV}$  data (two third of the total amount of data collected in 2012) were presented. The observation of a Higgs-like particle is confirmed in the  $H \rightarrow \gamma\gamma$  channel alone ( $6.1\sigma$  significance), and the fermionic decay channels are not yet sensitive to the Standard Model Higgs boson, though they are close.

When combining the  $H \rightarrow ZZ^{(*)}$  and  $H \rightarrow \gamma\gamma$  channels, the mass of the particle is  $125.2 \pm 0.3(\text{stat}) \pm 0.6(\text{syst})\text{GeV}$ , and the signal strength for this mass when combining the five different channels is  $1.35 \pm 0.19(\text{stat}) \pm 0.15(\text{syst})$ .

Different spin and parity hypotheses for this boson were tested, and the spin 2 and spin  $0^-$  tend to be disfavored by data.

---

<sup>(2)</sup> The polar angle  $\theta^*$  of the photons is computed with respect to some given reference axis in the resonance rest frame where the reference axis is the  $z$ -axis of the Collins-Soper frame here.

## REFERENCES

- [1] ATLAS COLLABORATION, *JINST*, **3** (2008) S08003.
- [2] CMS COLLABORATION, *JINST*, **3** (2008) S08004.
- [3] ATLAS COLLABORATION, *Phys. Lett. B*, **716** (2012) 1, arXiv:1207.7214[hep-ex].
- [4] CMS COLLABORATION, *Phys. Lett. B*, **716** (2012) 30, arXiv:1207.7235[hep-ex].
- [5] RESCIGNO M. on behalf of the ATLAS COLLABORATION, *Higgs couplings from ATLAS*, talk presented at this conference.
- [6] ATLAS COLLABORATION, *Updated results and measurements of properties of the new Higgs-like particle in the four lepton decay channel with the ATLAS detector*, ATLAS-CONF-2012-169.
- [7] ATLAS COLLABORATION, *Observation and study of the Higgs boson candidate in the two photon decay channel with the ATLAS detector at the LHC*, ATLAS-CONF-2012-168.
- [8] ATLAS COLLABORATION, *Update of the  $H \rightarrow WW^{(*)} \rightarrow e\nu\mu\nu$  analysis with  $13.0\text{fb}^{-1}$  of data collected with the ATLAS detector*, ATLAS-CONF-2012-158.
- [9] ATLAS COLLABORATION, *Search for the Standard Model Higgs boson in  $H \rightarrow \tau^+\tau^-$  decays in proton-proton collisions with the ATLAS detector*, ATLAS-CONF-2012-160.
- [10] ATLAS COLLABORATION, *Search for the Standard Model Higgs boson produced in association with a vector boson and decaying to bottom quarks with the ATLAS detector*, ATLAS-CONF-2012-161.
- [11] ATLAS COLLABORATION, *An update of combined measurements of the new Higgs-like boson with high mass resolution channels*, ATLAS-CONF-2012-170.